

## XPS CHARACTERIZATION OF METAL-OXIDE NANOCOLUMN ARRAYS VIA ANODIZING Al/Nb/Mo METAL LAYERS

<sup>1</sup>Maria BENDOVA, <sup>1,2</sup>Jan PRASEK, <sup>1</sup>Alexander MOZALEV

<sup>1</sup>Department of Microelectronics, Faculty of Electrical Engineering and Communication, Brno University of Technology, Brno, Czech Republic, EU, [bendova@vut.cz](mailto:bendova@vut.cz), [mozalev@vut.cz](mailto:mozalev@vut.cz)

<sup>2</sup>CEITEC – Central European Institute of Technology, Brno University of Technology, Brno, Czech Republic, EU, [prasek@vut.cz](mailto:prasek@vut.cz)

<https://doi.org/10.37904/nanocon.2023.4751>

### Abstract

Molybdenum oxides exhibit numerous electronic properties thanks to the ability of Mo to possess various oxidation states and coordinations. Molybdenum oxides are thus attractive for applications in energy storage, conversion, electrochromic, gas sensing, or superconducting devices. The nanostructuring of molybdenum oxides, controlled through the preparation conditions, is advantageous for enhancing the material's properties. The so-called porous-anodic-alumina (PAA)-assisted anodizing, based on the anodic oxidation of a metal layer through a PAA overlayer, may also be a way to grow molybdenum-oxide nanocolumn arrays if their stability in water-containing electrolytes can be secured. To take on the challenge, we envisioned mixing MoO<sub>x</sub> with the oxide of a different metal (Nb), by placing a thin interlayer of Nb between the Al and Mo in the precursor thin-film stack. The arrays were prepared from the magnetron-sputtered Al/Nb/Mo trilayers by anodizing at 46 V, then re-anodizing to 180 V, followed by selective dissolution of the PAA overlayer. Detailed XPS characterization confirmed that various Mo species were present in the column material, with a total amount of Mo reaching 16 at.% (Mo+Nb = 100%). The fitting of the narrow-scan Nb 3d and Mo 3d spectra showed that Mo<sup>6+</sup>, Mo<sup>5+</sup>, and Mo<sup>4+</sup>, in various ratios, were present at the column surface material, whereas Nb<sub>2</sub>O<sub>5</sub> was almost entirely stoichiometric. Further investigation is underway to understand the formation-structure-morphology relationship and explore the functional properties of the novel nanoarrays.

**Keywords:** Anodizing, porous anodic alumina, molybdenum oxides niobium pentoxide

### 1. INTRODUCTION

The nanostructuring of metal oxides is beneficial for many applications since the surface-to-volume ratio becomes more significant and the distance to the surface is shortened [1]. Various synthesis approaches have been developed to obtain one-dimensional nanostructures like nanowires or nanocolumns anchored to the substrate. They include wet chemical treatments, physical and chemical vapor deposition, and electrodeposition [1,2]. An alternative approach has been developed and applied for growing metal-oxide nanocolumn arrays: the so-called PAA-assisted anodizing [3]. It utilizes a bilayer of a thin film of aluminum deposited on a thin film of another valve metal, e.g., Ta, Nb, W, Ti, Hf, or Zr. First, the Al layer is transformed into porous anodic alumina (PAA) by anodizing in an acidic electrolyte. This is followed by anodic oxidation of the underlying metal locally through the PAA's barrier layer. In this way, short oxide nanoprotusions of the underlying metal are formed, mixed with alumina to some extent. Further, re-anodizing to a higher voltage may prolong the oxide protrusions inside the alumina pores. Metal-oxide nanocolumns, upright standing on a substrate, guided by the morphology of the initially formed PAA layer, may thus be created.

Molybdenum oxides (MoO<sub>x</sub>) possess a wide range of electrical properties owing to various oxidation states and coordinations of Mo cations [4,5]. Stoichiometric MoO<sub>3</sub> behaves as an insulator, whereas the almost

stoichiometric  $\text{MoO}_{3-\delta}$  (with  $\delta < 0.03$ ), the defective  $\text{MoO}_{3-\delta}$  (with  $0.03 < \delta < 0.11$ ), and the Magnéli phases are *n*-type semiconductors.  $\text{MoO}_2$  and  $\text{Mo}_2\text{O}$  reportedly show metallic behavior. This variety results in broad application areas, including energy storage and conversion, electrochromic, gas sensing, or superconducting devices [5]. Until now, no reports have been on the successful preparation of  $\text{MoO}_x$  nanocolumn arrays by the PAA-assisted anodizing of molybdenum. The main obstacles are the electrochemical behavior of molybdenum and the instability of molybdenum oxides in anodizing electrolytes [4,6]. A possible way to overcome these difficulties could be mixing molybdenum oxide with another metal oxide, e.g., niobium pentoxide, which could be done by using an Al/Nb/Mo trilayer for the PAA-assisted anodizing instead of an Al/Mo bilayer. In addition, mixing the two oxides in the column material may improve their electrical, electrochemical, or optical properties.

In this work, we have anodically processed an Al/Nb/Mo trilayer, having 25 nm Nb as the interlayer, to synthesize novel  $\text{MoO}_x\text{-Nb}_2\text{O}_5$  nanostructure arrays. The chemical composition of the arrays, mainly the Mo:Nb ratio and stoichiometry of the oxides, has been examined by X-ray photoelectron spectroscopy (XPS).

## 2. EXPERIMENTAL PART

### 2.1. Sample preparation

The precursor Al/Nb/Mo thin-film trilayer was prepared on an oxidized Si wafer by the magnetron sputter-deposition of a 200-nm thick Mo layer followed by a 25-nm thick Nb layer and by a 1- $\mu\text{m}$  thick Al layer using Mo (99.95%), Nb (99.95%), and Al (99.999%) targets, respectively. 1 cm  $\times$  1 cm samples cut from the wafer were galvanostatically anodized at a steady-state voltage of 46 V in 0.6 M oxalic acid at room temperature. For selected samples, re-anodizing was carried out in a borate buffer (0.5 M  $\text{H}_3\text{BO}_3$ /0.05 M  $\text{Na}_2\text{B}_4\text{O}_7$ ) to a more anodic voltage, up to 180 V. The PAA overlayer was partially or fully selectively etched away in  $\text{Cr}_2\text{O}_3/\text{H}_3\text{PO}_4$ -based etchant [7] to obtain the 'PAA-half-etched' or 'PAA-free' samples. Field-emission SEM, utilizing an InBeam detector for secondary electrons, was employed to examine the morphology of the anodic films.

### 2.2. XPS characterization

XPS analysis was carried out in a Kratos Axis Ultra DLD spectrometer using a monochromatic Al K $\alpha$  source. The X-ray emission power was 150 W with a 15 kV accelerating voltage focused to 300  $\mu\text{m}$   $\times$  700  $\mu\text{m}$ . The emitted electrons were detected at fixed pass energies of 160 eV for the survey spectra and 20 eV for the high-resolution spectra. The Kratos charge neutralizer system was used for all specimens.

The spectra were analyzed using CasaXPS. GL(30) profiles were used for all components except the metallic core lines of Nb 3d, for which asymmetric profiles in the form of LA(1.2,3.3,12) were applied. A standard Shirley background was used in all fitted spectra. Spectra from all samples have been charge-corrected to give the adventitious C 1s spectral component (C–C, C–H) binding energy of 284.8 eV. The deconvolution of C 1s spectra was performed as described elsewhere [3].

## 3. RESULTS AND DISCUSSION

### 3.1. Film morphology (SEM)

The PAA-assisted anodizing of the Al/25-nm Nb/Mo trilayer at 46 V, followed by PAA dissolution, yields an array of ~70-nm high 'nanogoblets' standing perpendicularly on the substrate (**Figure 1b**), surrounded by a network of Al residues. An SEM image of a cross-section of the same sample before the PAA dissolution is shown in **Figure 1a**, where the shape of the oxide grown below the nanogoblets is visible. Further re-anodizing to 180 V (see the SEM image in **Figure 1c**) leads to the elongation of the nanoprotusions to 560 nm and the expansion of the lower oxide parts into a continuous bottom-oxide layer. The following PAA etching yields an array of oxide nanocolumns vertically aligned on the bottom-oxide layer (**Figure 1d**). Thus, adding a 25-nm

thick Nb interlayer between the Al and Mo layers helps protect the column material from dissolution in the used electrolytes and enables a successful PAA-assisted growth of a molybdenum-oxide-based nanoarray.

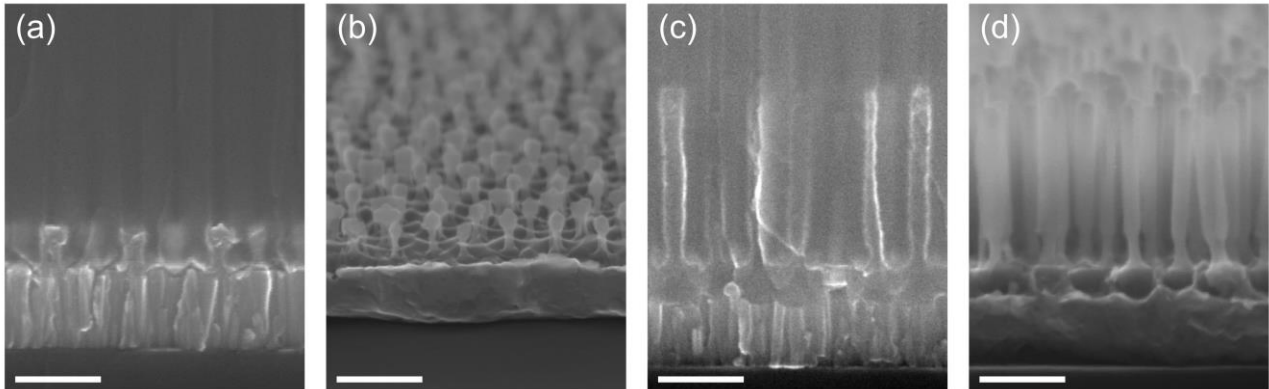


**Figure 1** SEM images showing cross-sections of (a,c) PAA-embedded and (b,d) PAA-free (a,b) anodized (nanogoblets) and (c,d) re-anodized (nanocolumn) arrays on  $\text{SiO}_2/\text{Si}$  substrates. All scale bars are 200 nm.

Based on the SEM observations, a schematic process for forming  $\text{MoO}_x\text{-Nb}_2\text{O}_5$  nanostructure arrays is described in **Figure 2**. Due to the thin Nb interlayer between the Al and Mo layers, we expect a composition gradient along the columns, indicated by the color gradient in the schematics. Three samples - the anodized PAA-free (**Figure 2e**), the re-anodized PAA-free (**Figure 2f**), and the re-anodized PAA-half-etched (**Figure 2g**) films - were subjected to a detailed XPS characterization.

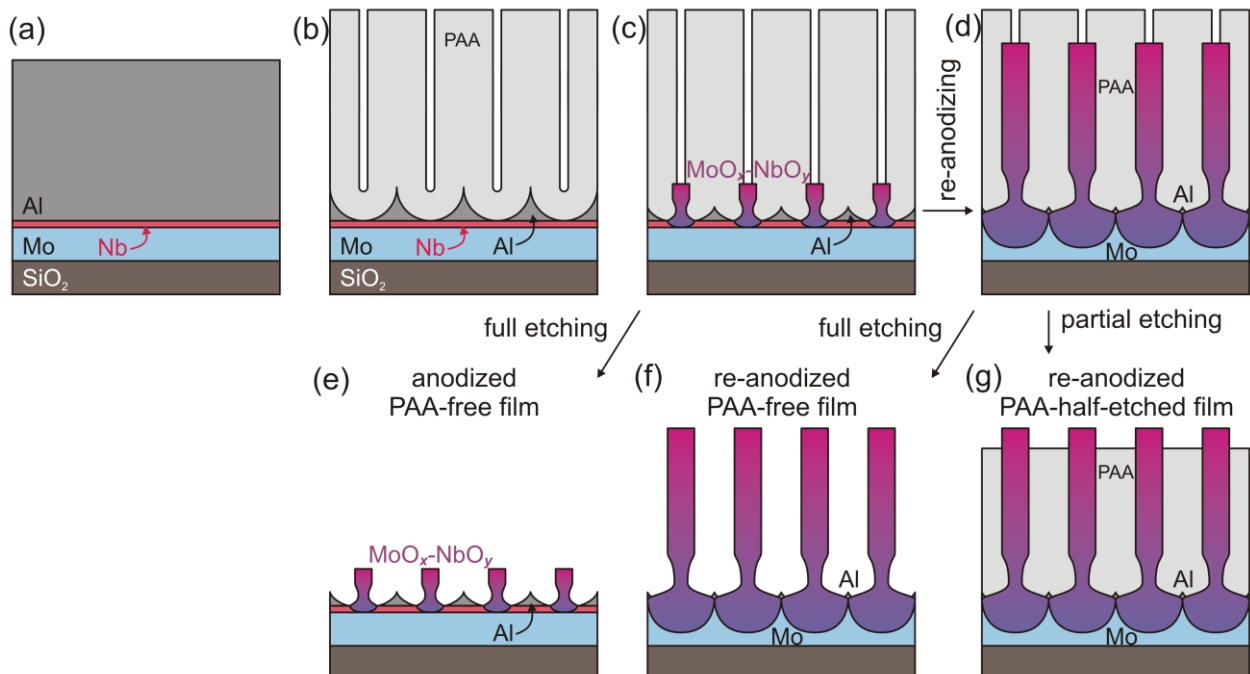


**Figure 2** Schematic process for forming the anodized and re-anodized  $\text{MoO}_x\text{-Nb}_2\text{O}_5$  nanoarrays: (a) the sputter-deposition of an Al/25-nm Nb/Mo trilayer onto an oxidized Si wafer, (b) the anodizing of the Al layer at 46 V to form a PAA film, (c) the anodizing of the Nb and Mo layers through the PAA barrier layer, (d) the re-anodizing of Nb and Mo layers to 180 V, (e) the anodizing followed possibly by full etching of the PAA overlayer to obtain the anodized PAA-free film and (f,g) the re-anodizing followed by (f) full or (g) partial etching of the PAA overlayer to obtain the re-anodized PAA-free or PAA-half-etched film, respectively

### 3.2. Film composition (XPS)

Examination of the chemical composition and bonding states at the surface layer of the anodized PAA-free, re-anodized PAA-free, and re-anodized PAA-half-etched films was performed by XPS. The presence of C, Nb, Mo, O, Al, P, and Cr was identified in the survey spectra, the last two elements being present due to the PAA dissolution in the  $\text{Cr}_2\text{O}_3/\text{H}_3\text{PO}_4$ -based etchant. Narrow-scan C 1s, Nb 3d, Mo 3d, O 1s, and Al 2p spectra were collected to perform quantitative analysis and reveal the bonding states. The experimental and fitted Nb 3d, Mo 3d, and Al 2p spectra are shown in **Figure 3**.

The Nb 3d spectra (**Figures 3a–c**) are fit with doublets of appropriately constrained peaks (Nb 3d<sub>5/2</sub> and 3d<sub>3/2</sub> with fixed peak separation energy of 2.75 eV and with a fixed intensity ratio of 3:2 [3]). The highest-intensity doublet, situated at the highest binding energy, is due to the presence of Nb<sup>5+</sup> cations [3]. The PAA-free samples also contain metallic Nb<sup>0</sup>, manifested by a doublet at the lowest binding energy, which separates the column bases [3]. The relative amount of the metallic Nb<sup>0</sup> is substantially smaller in the re-anodized anodic film than in the anodized film (2% vs. 21% of all Nb species), which agrees with the SEM observations (**Figure 1**). In the PAA-free films, also a low-intensity doublet is present, shifted to -1.8 eV from the Nb<sup>5+</sup> component, which is attributed to Nb<sup>4+</sup> cations [3] (the Nb<sup>2+</sup> cations in the anodized PAA-free film are most likely related with the metallic residues). The ratio of Nb<sup>5+</sup>:Nb<sup>4+</sup> cations is 96.5:3.5 and 98:2 in the anodized and re-anodized PAA-free films, respectively, suggesting the presence of a substoichiometric Nb<sub>2</sub>O<sub>5</sub> at the surface layer of the columns, as was disclosed earlier for some other metal oxides [3,7]. On the other hand, the re-anodized PAA-half-etched film shows only the Nb<sup>5+</sup> doublet in the Nb 3d spectrum (**Figure 3c**), meaning that the column tops contain stoichiometric Nb<sub>2</sub>O<sub>5</sub>.

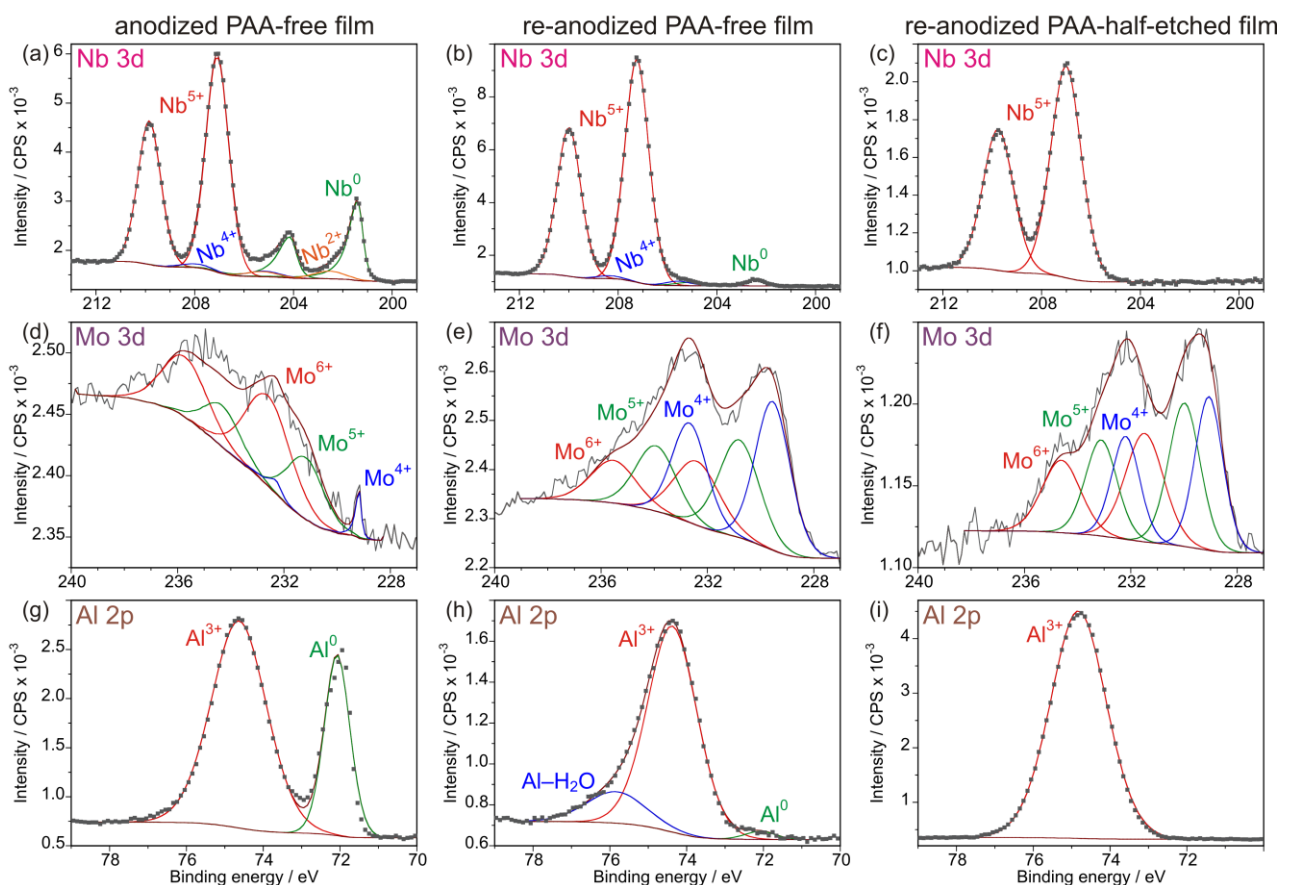


**Figure 3** Experimental and fitted XPS spectra of the surface of the (a,d,g) anodized PAA-free, (b,e,h) re-anodized PAA-free, and (c,f,i) re-anodized PAA-half-etched anodic films. In rows (a–c) Nb 3d, (d–f) Mo 3d, and (g–i) Al 2p high-resolution spectra are shown.

The *Mo 3d spectra* of the anodic films (**Figure 3d–f**) are also fit with constrained doublets ( $\text{Mo } 3d_{5/2}$  and  $3d_{3/2}$  with fixed peak separation energy of 3.13 eV and with a fixed intensity ratio of 3:2 [8,9]). The spectrum of the anodized PAA-free film is fit with two intense doublets assigned to  $\text{Mo}^{6+}$  and  $\text{Mo}^{5+}$  cations [8], with a mutual ratio of 64:36. In addition, a small sharp peak is present at 229.2 eV with FWHM of 0.2 eV, which might be due to  $\text{Mo}^{4+}$  oxidation state [8]. The spectrum of the re-anodized PAA-free film is composed of three doublets of similar intensities, assigned to  $\text{Mo}^{6+}$ ,  $\text{Mo}^{5+}$ , and  $\text{Mo}^{4+}$  cations in a ratio of 24:33:43. The spectrum of the re-anodized PAA-half-etched film has a similar composition. However, the ratio of cations is 32:35:33, indicating a slightly different oxide composition at the column tops. Thus, the anodic oxide composing the surface layer of the column material contains Mo cations of several oxidation states.

The fitted Nb 3d and Mo 3d narrow-scan spectra were also used for quantitative analysis to obtain the Mo content (providing that  $\text{at.}(\text{Mo}+\text{Nb})=100\%$ ). In the case of the anodized PAA-free film, containing a substantial amount of metallic Nb surrounding the nanogoblets, the metallic contribution was subtracted to reveal the Mo content in the surface layer only. The nanogoblets thus possess 4.4 at.% Mo, whereas the nanocolumns have an average of 8.5 at.% Mo. The column tops accumulate the highest molybdenum concentration of 16.1 at.%. The low Mo content in the nanogoblet composition means that the anodizing affects only a tiny part of the Mo layer.

In contrast, a relatively thicker Mo layer becomes involved in the film formation during the re-anodizing, as also seen in SEM images of **Figure 1**. One may expect a relatively higher Nb content at the column tops (as indicated by the color gradient in the schematic images, **Figure 2**), since the anodizing front reaches the Nb interlayer earlier than the Mo underlayer. However, the surface concentration of Mo at the column tops appeared to be unexpectedly higher (16.1 at.%) compared with the average surface composition (8.5 at.% Mo). This finding implies that the migration of  $\text{Mo}^{n+}$  cations occurs at a faster rate relative to the  $\text{Nb}^{5+}$  cations during the column growth.

The *Al 2p spectra* (**Figures 3g–i**) are fit with singlet peaks. A high-intensity peak associated with  $\text{Al}_2\text{O}_3$  is present in all spectra. A narrower lower-intensity  $\text{Al}^0$  peak is additionally found in the spectrum of the anodized and re-anodized PAA-free films and a broader low-intensity peak, shifted to +1.5 eV from the  $\text{Al}_2\text{O}_3$  peak, is seen in the spectrum of the re-anodized PAA-free film, which is attributed to a hydrated  $\text{Al}_2\text{O}_3$  [10]. The metallic Al (and part of the alumina peak) is attributed to Al metal residues, covered with native oxide, residing between the nanogoblets and, to a smaller extent, the nanocolumns. The metallic contributions were subtracted from the Al 2p and Nb 3d spectra of the anodized and re-anodized PAA-free films to obtain an approximate amount of alumina at the surface of the oxide nanocolumns. For Al, the corresponding native oxide was also subtracted [11]. In this way, 24, 57, and 96 at.% of Al were obtained for the anodized PAA-free, re-anodized PAA-free, and re-anodized PAA-half-etched films, respectively (providing that  $\text{at.}(\text{Al}+\text{Nb}+\text{Mo})=100\%$ ). The amount of Al in the columns of the PAA-free films is comparable with the Al amounts obtained for Se-doped  $\text{Nb}_2\text{O}_5$  PAA-assisted nanocolumns reported in a previous work [7], ranging ~50–80 at.% Al. The extraordinarily high amount of Al in the PAA-half-etched film is explained by the dominating presence of PAA surrounding the column tops.

The chemical composition of the surface layer of the nanogoblets and nanocolumns is thus substoichiometric  $\text{Nb}_2\text{O}_5$ , mixed with  $\text{Al}_2\text{O}_3$  and complemented by various molybdenum oxides; the molybdenum concentration increasing towards the tops of the nanocolumns. The interior of the columns is most probably alumina-free molybdenum-niobium mixed oxide [3].

#### 4. CONCLUSIONS

For the first time, the 25-nm Nb/Mo layers were processed via PAA-assisted anodizing and re-anodizing. Adding a 25-nm thick Nb interlayer between the Al and Mo layers enabled the successful growth of chemically stable molybdenum-oxide-containing nanogoblet and nanocolumn arrays. The XPS analysis revealed that the surface layer of the nanogoblets and nanocolumns contained respectively 4.4 and 8.5 at.% Mo in the form of

various molybdenum oxides ( $\text{Mo}^{n+}$  cations with 6+, 5+, and 4+ oxidation states), mixed with substoichiometric  $\text{Nb}_2\text{O}_5$  and also  $\text{Al}_2\text{O}_3$  originating from the alumina cell walls.

The mixing at the nanoscale of relatively small amounts of molybdenum oxides with some other semiconducting metal oxides may reportedly substantially impact their fundamental properties governing the electrical, electronic, and electrochemical behavior of such oxides, with a potential for emerging energy storage applications [6]. Functional properties of the nanoarrays developed here will be the subject of future works.

## ACKNOWLEDGEMENTS

**The research leading to these results was supported by GACR grant no. 23-07848S. We acknowledge the use of CzechNanoLab Research Infrastructure supported by MEYS CR (LM2018110).**

## REFERENCES

- [1] DEVAN, R.S.; PATIL, R.A.; LIN, J.-H.; MA, Y.-R. One-dimensional metal-oxide nanostructures: recent developments in synthesis, characterization, and applications. *Advanced Functional Materials*. 2012, vol. 22, pp. 3326–3370.
- [2] LEE, W.; PARK, S.-J. Porous anodic aluminum oxide: anodization and templated synthesis of functional nanostructures. *Chemical Reviews*. 2014, vol. 114, pp. 7487–7556.
- [3] MOZALEV, A.; VÁZQUEZ, R.M.; BITTENCOURT, C.; COSSEMENT, D.; GISPERT-GUIRADO, F.; LLOBET, E.; HABAZAKI, H. Formation–structure–properties of niobium-oxide nanocolumn arrays via self-organized anodization of sputter-deposited aluminum-on-niobium layers. *Journal of Materials Chemistry C*. 2014, vol. 2, pp. 4847–4860.
- [4] ALVES de CASTRO, I.; DATTA, R.S.; OU, J.Z.; CASTELLANOS-GOMEZ, A.; SRIRAM, S.; DAENEK, T.; KALANTAR-ZADEH, K. Molybdenum oxides – from fundamentals to functionality. *Advanced Materials*. 2017, vol. 29, 1701619 (31pp).
- [5] CONCEPCIÓN, O.; de MELO, O. The versatile family of molybdenum oxides: synthesis, properties, and recent applications. *Journal of Physics: Condensed Matter*. 2023, vol. 35, 143002 (26pp)
- [6] ELKHOLY, A.E.; DUIGNAN, T.T.; SUN, X.; ZHAO, X.S. Stable  $\alpha\text{-MoO}_3$  electrode with a widened electrochemical potential window for aqueous electrochemical capacitors. *ACS Applied Energy Materials*. 2021, vol. 4, pp. 3210–3220.
- [7] KAMNEV, K.; BENDOVA, M.; PYTLICEK, Z.; PRASEK, J.; KEJÍK, L.; GÜELL, F.; LLOBET, E.; MOZALEV, A. Se-doped  $\text{Nb}_2\text{O}_5\text{-Al}_2\text{O}_3$  composite-ceramic nanoarrays via the anodizing of Al/Nb bilayer in selenic acid. *Ceramics International*. 2023, vol. 49, pp. 34712–34725.
- [8] SPEVACK, P.A.; McINTYRE, N.S. Thermal reduction of  $\text{MoO}_3$ . *Journal of Physical Chemistry*. 1992, vol. 96, pp. 9029–9035.
- [9] BIESINGER, M.C. *X-ray Photoelectron Spectroscopy (XPS) Reference Pages, Molybdenum* [online]. 2009–2021 [viewed: 2023-08-16]. Available from: <http://www.xpsfitting.com/search/label/Molybdenum>
- [10] BIESINGER, M.C. *X-ray Photoelectron Spectroscopy (XPS) Reference Pages, Aluminum* [online]. 2009–2021 [viewed: 2023-08-17]. Available from: <http://www.xpsfitting.com/search/label/Aluminum>.
- [11] STROHMEIER, B.R. An ESCA method for determining the oxide thickness on aluminum alloys. *Surface and Interface Analysis*. 1990, vol. 15, pp. 51–56.